ACCOUNTS
of chemical research

Mapping the Landscape of RNA Dynamics with NMR Spectroscopy

JÖRG RINNENTHAL, JANINA BUCK, JAN FERNER,
ANNA WACKER, BORIS FÜRTIG, AND HARALD SCHWALBE*

Institute for Organic Chemistry and Chemical Biology, Center for Biomolecular Magnetic Resonance, Johann Wolfgang Goethe-University, Max-von-Laue-Strasse 7, D-60438 Frankfurt/Main, Germany

RECEIVED ON MAY 18, 2011

CONSPECTUS

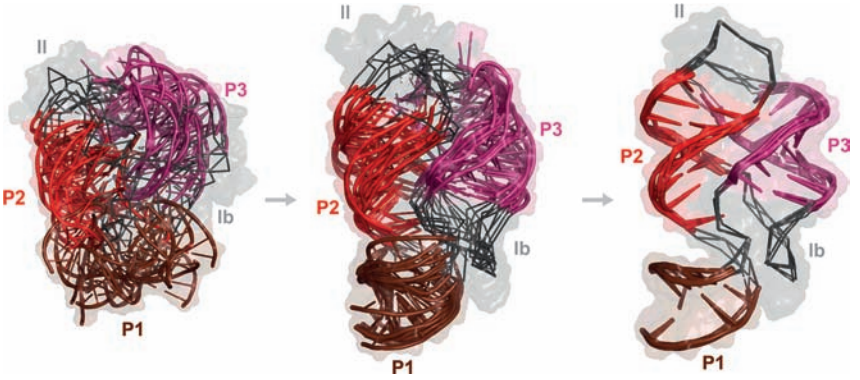

Among the three major classes of biomacromolecules (DNA, RNA, and proteins) RNA's pronounced dynamics are the most explicitly linked to its wide variety of functions, which include catalysis and the regulation of transcription, translation, and splicing. These functions are mediated by a range of RNA biomachinery, including such varied examples as macromolecular noncoding RNAs, microRNAs, small interfering RNAs, riboswitch RNAs, and RNA thermometers. In each case, the functional dynamics of an interconversion is characterized by an associated rate constant. In this Account, we provide an introduction to NMR spectroscopic characterization of the landscape of RNA dynamics. We introduce strategies for measuring NMR parameters at various time scales as well as the underlying models for describing the corresponding rate constants.

RNA exhibits significant dynamic motion, which can be modulated by (i) intermolecular interactions, including specific and nonspecific binding of ions (such as Mg^{2+} and tertiary amines), (ii) metabolites in riboswitches or RNA aptamers, and (iii) *macromolecular interactions* within ribonucleic protein particles, including the ribosome and the spliceosome. Our understanding of the nature of these dynamic changes in RNA targets is now being incorporated into RNA-specific approaches in the design of RNA inhibitors. Interactions of RNA with proteins, other RNAs, or small molecules often occur through binding mechanisms that follow an induced fit mechanism or a conformational selection mechanism, in which one of several populated RNA conformations is selected through ligand binding.

The extent of functional dynamics, including the kinetic formation of a specific RNA tertiary fold, is dependent on the messenger RNA (mRNA) chain length. Thus, during de novo synthesis of mRNA, both in prokaryotes and eukaryotes, nascent mRNA of various lengths will adopt different secondary and tertiary structures. The speed of transcription has a critical influence on the functional dynamics of the RNA being synthesized.

In addition to modulating the local dynamics of a conformational RNA ensemble, a given RNA sequence may adopt more than one global, three-dimensional structure. RNA modification is one way to select among these alternative structures, which are often characterized by nearly equal stability, but with high energy barriers for conformational interconversion. The refolding of different secondary and tertiary structures has been found to be a major regulatory mechanism for transcription and translation. These conformational transitions can be characterized with NMR spectroscopy, for any given RNA sequence, in response to external stimuli.

Introduction

Among all the biophysical methods, nuclear magnetic resonance (NMR) spectroscopy stands out in its ability to characterize conformational dynamics at atomic resolution over time scales ranging from picoseconds to seconds. Recent progress is now paving the way toward performing NMR

Published on the Web 09/06/2011 www.pubs.acs.org/accounts
10.1021/ar200137d

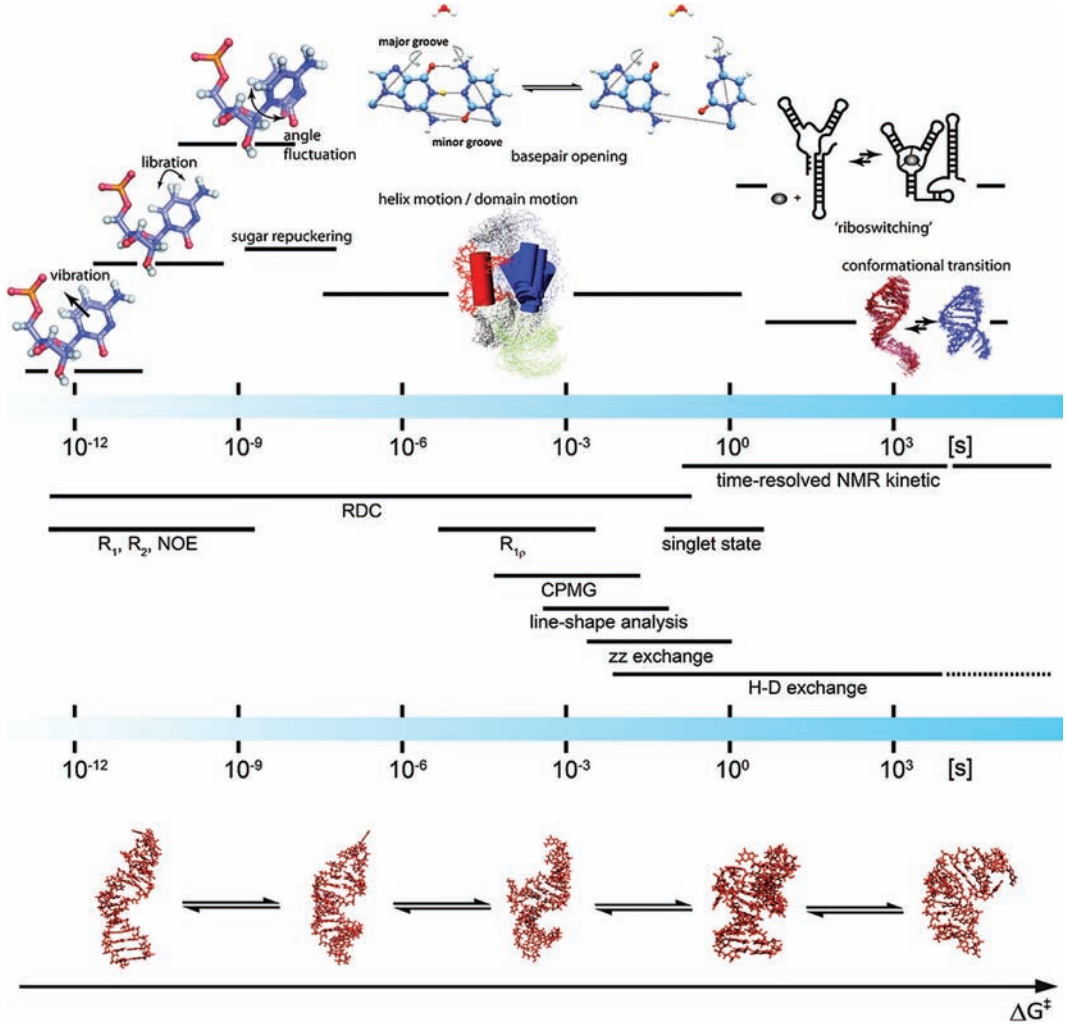

FIGURE 1. Time scales of different dynamic processes in RNA (above) and corresponding NMR methods for their investigation (middle). (Below) Transitions of different RNA conformations occur on different dynamic time scales dependent on the energy barrier $\Delta G^{\ddagger}$ that has to be overcome. Some of these conformations are binding competent to a special ligand while others are not.

experiments on RNAs in situ to further determine the influence of intracellular factors on the structure and dynamics of RNAs.[1] Depending on the time scale of the dynamic processes under investigation, specific NMR spectroscopic techniques are applied to obtain spatially resolved information (Figure 1). In the following sections, we describe the application of NMR spectroscopy in light of the rate constants of the respective dynamic transitions and provide a link to discuss the associated underlying biochemical functions of RNA.

Fast Dynamics: Bond Librations and Angular Fluctuations on Time Scales of Picoseconds to Nanoseconds

NMR spectroscopy is able to detect dynamics arising from internal motions that are faster than the global rotational correlation time τ_c (order, 1−40 ns; size-dependent) of the RNA. Information on fast dynamics is obtained from analysis of spin−lattice (R_1) and spin−spin (R_2) relaxation rates and the heteronuclear nuclear Overhauser effects (NOEs) of ^{13}C, ^{15}N, and ^{31}P nuclei. In the case of RNA, solvent exchange-protected imino protons involved in base-pairing are accessible to relaxation analysis.[2] By characterizing the relaxation of C6−H6 (pyrimidines), C8−H8 (purines), and C1′−H1′ sites, non-base-paired nucleotides like those in noncanonical regions of RNA can also be monitored. Among others, the U1A-binding RNA domain in the free and protein-bound form,[3,4] various transactivation-response element (TAR) RNA ligand complexes,[5,6] Smaug recognition element (SRE)-RNA in the free form and complexed with its protein binding partner VTS1p-SAM,[7] and cUUCGg tetraloop 14mer RNA[8,9] have been studied. Internal motions such as bond vibrations and librations are interpreted using an approach

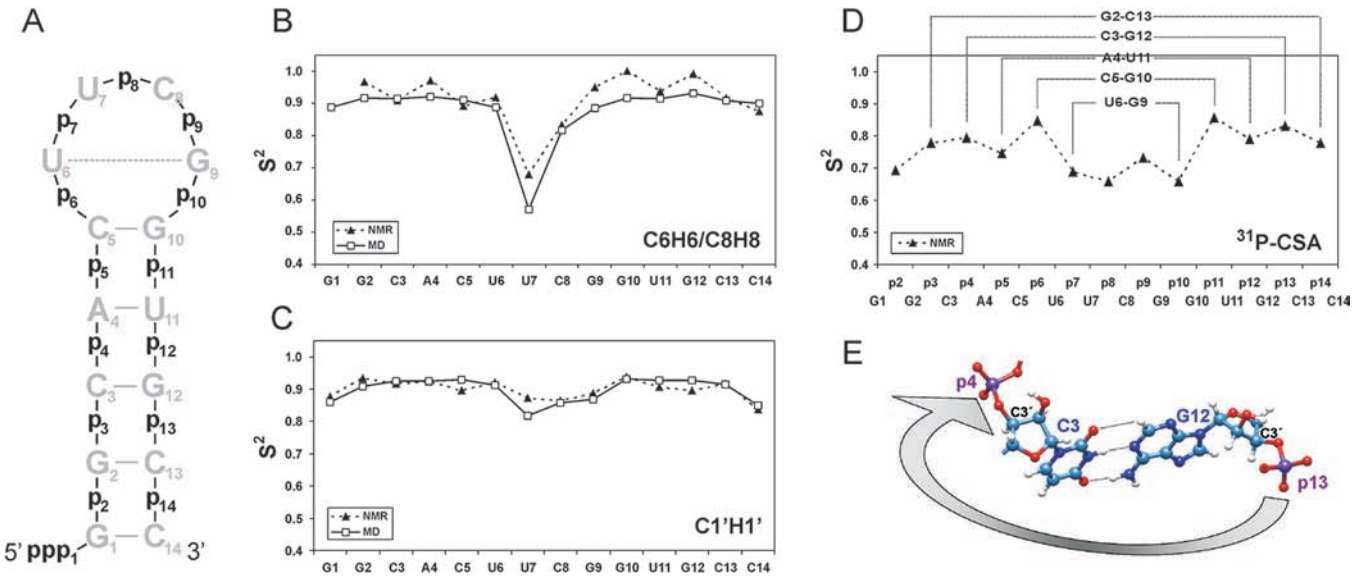

FIGURE 2. Fast time scale dynamics of the cUUCGg tetraloop 14mer RNA. (A) Secondary structure. (B, C) S^2_{LS} order parameters for nucleobases (B) and ribose moieties (C) extracted from ^{13}C relaxation data and MD trajectories. (D) S^2_{LS} order parameters for the phosphodiester backbone extracted from ^{31}P relaxation data measured using a perdeuterated 14mer sample. (E) Three-dimensional representation highlighting the dynamic link between p4 and p13 mediated by the C3-G12 base pair.

termed "model-free formalism".[10] The Lipari–Szabo order parameter S^2_{LS} describes the extent of internal motion, which becomes more pronounced the more S^2_{LS} deviates from unity ($0 \le S^2_{LS} \le 1$). For $S^2_{LS} = 1$, motion of the bond vector arises solely from the overall rotational tumbling of the RNA. Akke et al. performed this type of analysis at 273 K on the N–H imino groups of the stem nucleobases of a 14mer RNA containing a cUUCGg tetraloop.[2] For essentially the same 14mer RNA (Figure 2A), ^{13}C relaxation data were analyzed for the C6–H6 (pyrimidines) and C8–H8 (purines) bond vectors of the nucleobases (Figure 2B) and the C1′–H1′ bond vectors of the sugar moieties (Figure 2C) at 298,[8,9] 317, and 325 K.[9] At 298 K, S^2_{LS} values for the stem were found to be 0.92–1. The terminal nucleobase C14 ($S^2_{LS} = 0.87$) and the loop nucleobases U7 ($S^2_{LS} = 0.68$) and C8 ($S^2_{LS} = 0.83$) were more flexible. The loop nucleobases U6 ($S^2_{LS} = 0.92$) and G9 ($S^2_{LS} = 0.95$), which are involved in wobble base pairing, were more rigid than the loop nucleobases U7 and C8. The order parameters of the C1′–H1′ bond vectors of the sugar moieties exhibited smaller variations at 298 K and ranged from 0.84 to 0.94. The S^2_{LS} values for the sugars and nucleobases were in agreement with order parameters extracted from molecular dynamics (MD) simulations.[9]

An interesting link between NMR-detected fast dynamics and chemical probing experiments has been reported for nucleotide-specific selective 2′-hydroxyl acylation analyzed by primer extension (SHAPE) chemistry.[11] Interestingly, SHAPE reactivity is correlated with the S^2_{LS} parameters of the C1′–H1′ bond vectors in TAR (Pearson correlation coefficient $R = 0.78$), U1A ($R = 0.89$), and T-SL4 RNA ($R = 0.73$), but not with solvent accessibility. Thus, SHAPE provides a valuable tool for mapping conformational dynamics, particularly for large RNAs, and NMR data contribute important insights for understanding the mechanistic aspects of SHAPE.

For the cUUCGg tetraloop RNA, fast phosphodiester backbone dynamics have been analyzed using ^{31}P relaxation.[12] Prior to this report, information was lacking due to restricted ^{31}P chemical shift dispersion and because dipolar ^{1}H–^{31}P relaxation depends on a number of remote ^{1}H atoms, requiring detailed knowledge of the structure of the phosphodiester backbone. However, using perdeuterated RNA, the ^{31}P chemical shift anisotropy (CSA) is the only remaining nuclear relaxation mechanism. A model-free analysis on the basis of R_1 and R_2 ^{31}P relaxation data (Figure 2D) results in S^2_{LS} values with substantial variation (0.66–0.86), with loop phosphates exhibiting higher flexibility than stem phosphates. Importantly, the order parameters of the phosphates on the 3′ end of a nucleotide are linked via base pairing (Figure 2E).

Fast Exchange: Conformational Dynamics with Rate Constants between 10^{-2} and 10^{-8} s^{-1}

In NMR, dynamic molecular motions slower than the overall rotational correlation time, in the range of nanoseconds to milliseconds, are typically called fast exchange. Several conformations with different chemical shifts give rise to a single

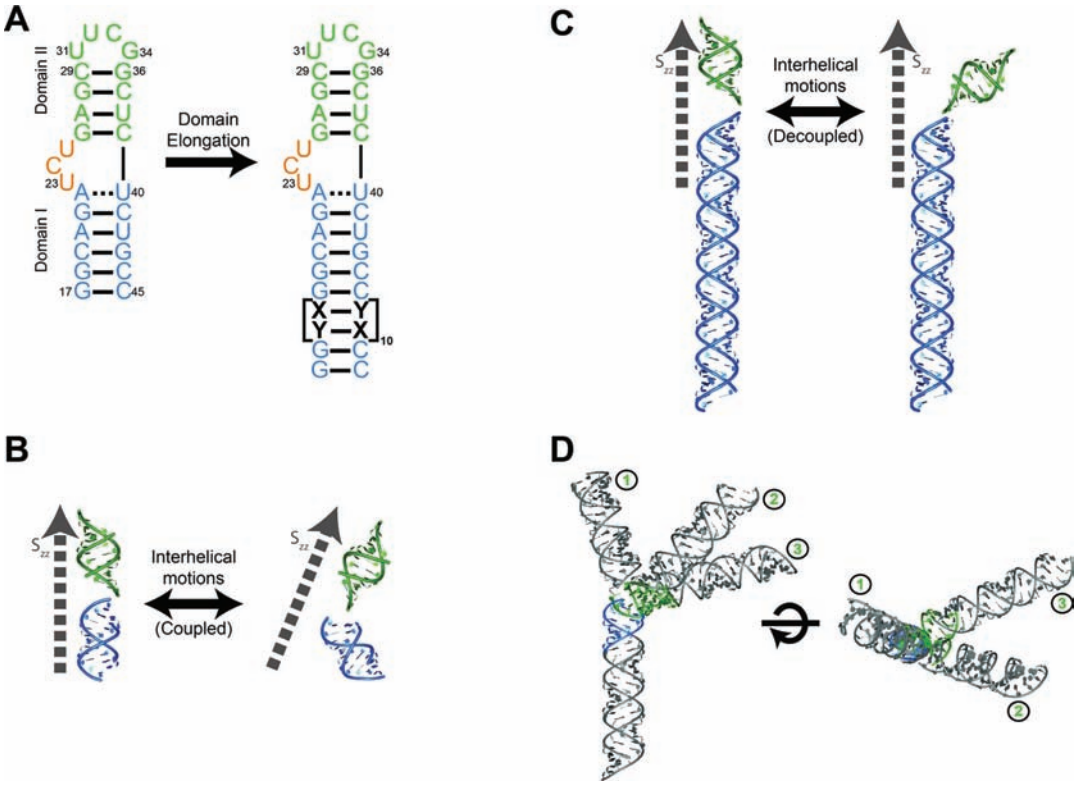

FIGURE 3. Decoupling of different motional modes in TAR RNA by domain elongation. (A) NMR invisible domain elongation of the loop-modified TAR RNA by AU (X = A; Y = U) or GC (X = G; Y = C) base pairs. (B) Interhelical domain motions lead to coupled changes in the principal axis of the rotational diffusion tensor. (C) The principal axis of the rotational diffusion tensor becomes insensitive to interdomain motions due to elongation of domain I. (D) The three TAR RNA conformations representing a structural ensemble based on the RDC fit.

NMR signal if conformational exchange is fast on the NMR time scale. Such fast chemical shift fluctuations can be characterized by various NMR methods, most frequently Carr–Purcell–Meiboom–Gill (CPMG), $R_{1\rho}$, or ΔR_{MQ} measurements. In CPMG measurements, a dependence of the R_2 rate on the length of the spin–echo indicates fast chemical exchange.[13–15] In most cases, a two-state conformational model is assumed for data analysis. From the dependence of the R_2 rates on the strength of the CPMG field, the exchange rate, the chemical shift difference between the two states, and their populations can be extracted. This method is suitable for determining chemical exchange over the range of 10^2–10^4 Hz. In $R_{1\rho}$ measurements, relaxation is analyzed under the influence of a constant spin-lock rf field.[16] By varying the strength and offset of the spin-lock rf field, exchange rates, populations, and chemical shift differences of the populated states can be obtained.[5,13,15] The $R_{1\rho}$ method is appropriate for investigating chemical exchange over the range of 10^3–10^5 Hz.

RNA/DNA fast exchange phenomena have been characterized using $R_{1\rho}$ or CPMG methods or a combination of both. Johnson et al. investigated the dynamic properties of a cGCAAg tetraloop 15mer RNA[17] that was selectively ^{13}C-labeled in the C2′ and C4′ positions of the sugar moieties, allowing dynamic analysis at two atomic sites per nucleotide. Chemical exchange was observed throughout the tetraloop with exchange rates (k_{ex}) of 20–40 kHz and chemical shift changes of 0.5–4 ppm. Strikingly, the exchange rates of the C2′ and C4′ resonances of the same sugar moiety as well as their temperature dependences were identical within the margin of error. This strongly suggests that the C2′ and C4′ of a sugar moiety are reporters of the same dynamic process that has been ascribed to a two-state sugar pucker interconversion, likely between the C3′- and C2′-endo conformations. Moreover, there was an indication of concerted conformational dynamics for the apical loop residues C6 and A7 and for the nucleotides G5 and A8. However, the possibility of internucleotide clustering of very similar exchange rates belonging to separate motional processes arising from simple coincidence cannot be rigorously excluded. This study exemplifies that detailed relaxation dispersion analysis of several spin-probes per nucleotide has the potential to identify and separate different motional modes as well as

concerted motions spanning two or even more nucleotides of one RNA.

Kloiber et al.[18] performed kinetic analysis of bistable RNAs under equilibrium conditions. Beside detailed analysis of two-state exchange by longitudinal exchange analysis, faster kinetics of one of the RNAs under investigation were analyzed by CPMG measurements at two different magnetic fields (500 and 800 MHz). The CPMG curves could be fitted according to a two-state model. The fit according to this model resulted in rate constants of 593 ± 133 (460 ± 268) s^{-1} for the two conformations. In addition, the chemical shift difference between the exchanging states is around 0.45 ppm (at an excited state population of 1%) and 0.8 ppm (at equimolar populations) for both conformers. Each conformation of the same RNA exhibits two additional exchange mechanisms on a slower time scale (2.70−3.79 Hz) that can be analyzed by longitudinal relaxation analysis.

The TAR RNA of HIV-1 has been subjected to extensive NMR dynamic characterization by the Al-Hashimi group.[19] Helix elongation of the TAR RNA (Figure 3A) allows separation of local fluctuations and helix-domain motions from overall global motions (Figure 3B, C), because the global correlation time is increased to allow separation of these different dynamics. The TAR RNA is divided into a stem (domain I, Figure 3A) and a loop domain (domain II, Figure 3A) that are connected by a flexible three-nucleotide bulge. Zhang et al.[19] identified fast fluctuations with amplitudes of $S_f^2 = 0.79-0.89$ (unrestricted $= 0 \leq S_f^2 \leq 1 =$ restricted), with the loop domain exhibiting slightly lower values than the stem domain. Through helix elongation, a second, slow motional mode could be identified for residues in the loop domain. Slow motions with amplitudes of $S_s^2 = 0.68-0.76$ and correlation times of $\tau_s = 1.5-1.9$ ns were detected in the loop domain, but were absent in the stem domain. This observation provides strong evidence that the slow motion represents helix reorientation, with the three-nucleotide bulge serving as a flexible hinge between the loop domain and the stem domain. This slow motional mode disappeared in the presence of the bulge-binding TAR ligand argininamide (ARG), consistent with the flexible hinge region becoming locked into a single conformation.

Another important method for investigating fast exchange is analysis of residual dipolar couplings (RDCs). Although in isotropic solution dipolar couplings average to zero, they are partially reintroduced in the presence of special alignment media; for RNA, phages are the preferred alignment medium. The size of an RDC measured in solution is scaled by the magnitude of dynamics faster than the inverse of the RDC. If the structure of a macromolecule is known, S^2_{RDC} order parameters can be obtained by analysis of the RDCs. By comparing S^2_{LS} and S^2_{RDC}, information can be obtained about dynamic processes between 10^1 and 10^8 Hz while the inequality $S^2_{RDC} \leq S^2_{LS}$ always applies.[20] Analysis of the $(S^2_{LS} - S^2_{RDC})$ difference is the only NMR spectroscopic method able to detect dynamics on a time scale of 10^5-10^8 Hz.[19,21,22]

An order tensor analysis based on RDCs has been performed for the TAR RNA of HIV-1, wherein large-amplitude helix motions were observed. Order tensor analysis determined values of $(S^2_{RDC})^{1/2} = \nu_{int}$ of $\sim$0.46,[23] which were considerably lower than those detected by spin relaxation $[(S_s^2 S_f^2)^{1/2} \approx 0.79]$.[19] This difference in amplitude can be assigned to supra-τ_c motions at 10^5-10^8 Hz. Slower motional modes (10^1-10^5 Hz) can be excluded, since line broadening, which would reveal those slower dynamics, was not observed. The obtained RDCs can be fitted by a model assuming at least three different interhelical conformations (Figure 3D).[23] Strikingly, helical twisting and bending motions appeared to be highly correlated. The twisting motions of domain I (angle γ) and domain II (angle α) and the bending motions (angle β) between domain I and domain II were linearly correlated in three-dimensional angular (Euler) space (α, β, γ).

To determine whether ligand binding to TAR RNA occurs via an induced fit or a conformational capture mechanism, binding studies have been performed with several different ligands. The induced fit model predicts a structural accommodation of the binding interface upon ligand encounter; the bound conformation is not present in the state representing free RNA. In contrast, the conformational capture model predicts an ensemble of many different conformations present in the free form. Depending on the specific ligand, one of these preexisting, but potentially low-populated structures is captured in the RNA-ligand complex.

Remarkably, structures of seven different TAR−ligand complexes traced a linear trajectory in three-dimensional Euler space that was very similar to the trajectory derived from the RDC dynamics of free TAR. This observation provides strong support for the conformational capture model, wherein the ligand binds a particular tertiary TAR structure existing in the ensemble of free TAR structures, thereby locking the RNA in one specific conformation. Each ligand might therefore bind to a different tertiary structure that is sampled in the conformational ensemble of the free

TAR. This is in agreement with the lack of RDC dynamics in the EI-TAR-ARG complex [$(S^2_{RDC})^{1/2} = \nu_{int}$ of $\sim 1.09 \pm 0.08$]. Similar observations have been made for other RNA–ligand complexes[24] as well as in the protein field.[22]

Intermediate Exchange: Conformational Dynamics in the Millisecond Time Regime Characteristic of Nonspecific Interactions

Chemical or conformational exchange processes in the millisecond range change the line shapes of NMR signals. Analysis of signals with line shape perturbations provides information about underlying exchange mechanisms. Currently, there are few reports on this phenomenon in RNA. We, therefore, refer the reader to protein examples for further study.[13,25]

Slow Exchange: Conformational Dynamics under 1 s^{-1}

Cross signals in nuclear Overhauser effect spectroscopy (NOESY) and rotating frame nuclear Overhauser effect spectroscopy (ROESY) can arise from spatial proximity of two different nuclei or from the slow exchange process of a single spin.[26] For biomacromolecules, these two cases cannot be distinguished in NOESY spectra. However, in ROESY experiments, exchange signals have a different sign than ROE signals and can be identified unambiguously.

Using a specific mixing time scheme comprising rapidly alternating NOE and ROE time periods, NOE/ROE cross peaks can be suppressed such that the residual cross peaks unambiguously originate from underlying [^{1}H–^{1}H] ZZ-exchange mechanisms.[27,28] [^{1}H–^{1}H] ZZ-exchange spectroscopy has been applied to investigate the ligand-binding kinetics of a theophylline-binding RNA aptamer.[29] This in-vitro-selected RNA aptamer requires Mg^{2+} (10 mM) for tight theophylline binding ($K_D \sim 300$ nM). In the absence of divalent metal ions, the K_D increases to ~ 7 mM at 25 °C. Thus, by choosing certain concentrations (0.8 mM RNA and 6.4 mM theophylline), nearly equal populations of the RNA–ligand complex and free RNA can be obtained. ZZ-Exchange measurements have been performed at various theophylline concentrations. The folding rates (k_f) followed a pseudo-first-order kinetic scheme in which $k_f = k_{on}[\text{theophylline}]_{free}$ with $k_{on} = 600 \pm 57\ M^{-1}\ s^{-1}$. In contrast, $k_{off} = 1.5 \pm 0.3\ s^{-1}$ was determined to be concentration-independent, as expected based on the mass action law model. Thus, RNA folding was directly coupled to ligand binding.

Another method for investigating slow exchange processes is to conduct ZZ-exchange measurements for nuclei with low gyromagnetic ratios (e.g., ^{15}N).[30] Because the NOE for these nuclei is small, cross signals almost exclusively occur due to exchange processes. However, exchange rates significantly smaller than the R_1 rates of these signals cannot be detected. Thus, using ZZ-exchange methods, exchange processes between 0.2 and 100 Hz can be observed.[27,31] Through preparation of singlet states, the T_1 relaxation time can be increased considerably (15–50 s), so that even slower exchange processes become observable.[32] This method is important in closing the gap between ZZ-exchange and conventional kinetic experiments.

Characterizing the Kinetics of Conformational Transitions Between Static Conformational States with Rate Constants of >10 s^{-1}

By performing NMR experiments in a fast and sequential manner, conformational transitions or reactions with kinetic rate constants $< 10\ s^{-1}$ can be observed. For fast kinetics, the NMR signal-to-noise ratio may be limiting, so that this time resolution can be achieved only in favorable cases with high sample concentrations and high spectral quality.[33–35] In such kinetic experiments, the time dependence of the product and/or educt signal intensity $I(t)$ is recorded. Assignment of respective NMR resonances is a prerequisite for interpretation of kinetic time traces. Thus, these states must be separately accessible to perform NMR assignment experiments.

Compared to the methods described above, kinetic measurements are performed under nonequilibrium conditions. Hence, kinetic measurements allow observation of kinetic processes even with extremely exergonic reactions, which is not possible with equilibrium methods. The ability to control initiation of the reaction is essential for kinetic measurements. Reactions can be triggered through rapid mixing of two solutions or by sudden release of a specific compound.[36] The release of "caged" compounds can be achieved photochemically by high light intensity irradiation of a sample (Figure 4).[36–38] Such methods are suited for kinetic examination of protein and RNA folding as well as protein–ligand and RNA–ligand interactions.

For example, physiologically relevant kinetic processes of RNA folding on the order of seconds can be observed in riboswitch RNAs. These RNA motifs are localized in the 5′-UTR and modulate gene expression upon binding of small metabolites. Structural reorganization of complex tertiary folds upon ligand binding causes the release (on-switch) or sequestration (off-switch) of the Shine–Dalgarno (SD) sequence in translation-regulating riboswitches. In

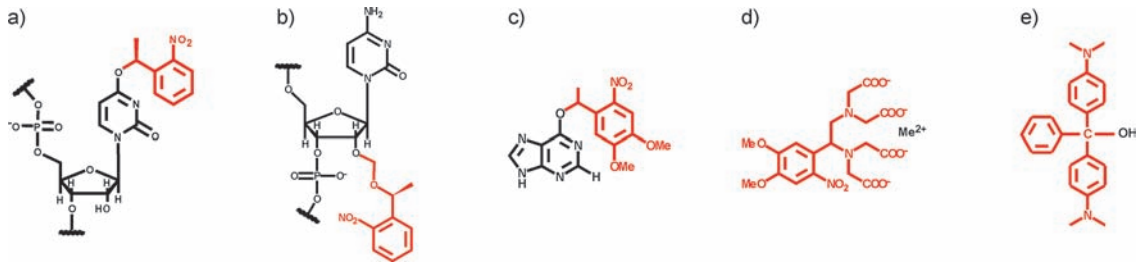

FIGURE 4. Photoprotecting strategies for defined initiation of RNA folding. (A) The Watson–Crick side of certain nucleotides in the RNA can be masked by photolabile groups [here: 1-(2-nitrophenyl)ethyl]. (B) The reactivity exerted by the 2′-OH group of the RNA, as in the case of ribozymes, can be protected to prevent premature execution of the chemical step. (C) Ligands inducing the folding of aptamers, as in riboswitches, can be protected in a manner that prevents binding. (D) Metal ions such as Ca^{2+} or Mg^{2+} that induce RNA folding by stabilizing tertiary interactions can be caged using photolabile EDTA-like compounds (here: dimethoxy-nitrophen). (E) Folding of RNA can also be triggered by changing the pH value within the sample (here: OH^- release by malachite green carbinol base).

transcription-regulating riboswitches, ligand binding causes formation of a terminator (off-switch) or antiterminator (on-switch) helix, leading to further transcription of mRNA or premature transcription termination. However, if the RNA polymerase successfully passes the point at which transcription termination can occur, the complete mRNA is transcribed independent of the folding of the riboswitch motif. Thus, the terminator hairpin must form within a certain period to induce transcription termination. Therefore, a detailed description of folding trajectories as well as the rate-determining factors of riboswitch folding is necessary for understanding the in vivo regulatory signal.

The guanine-sensing riboswitch of the *xpt-pbuX* operon belongs to the class of transcriptional off-switches. Time-resolved NMR spectroscopic studies on the ligand-induced folding kinetics of the guanine riboswitch aptamer domain (GSR^{apt}) have been performed.[37] In this study, the folding reaction was triggered by light-induced release of hypoxanthine from a photocaged precursor. A combination of selective RNA isotope labeling and NMR x-filter techniques yielded sufficient spectral and temporal resolution for kinetic analysis of individual RNA imino resonances, thereby providing site-resolved information on GSR^{apt} folding. Interestingly, individual folding rates clustered into two classes. Nucleotides of the ligand-binding core and the ligand itself exhibited half-lives ($t_{1/2}$) of 18.9–23.6 s. In addition, a slower process ($t_{1/2} = 27.1–30.7$ s) was observed for nucleotides in helix P2 and the long-range tertiary loop–loop region (L2 and L3) of the RNA. Moreover, line-broadening effects were observed for the signals of low-affinity ligands (e.g., adenine binding to GSR^{apt}) in the presence of GSR^{apt}, but not in the presence of a similar GSR construct lacking part of the core domain and the P1 helix. Thus, the core domain and/or the P1 helix were determined to be involved in nonspecific ligand binding on a fast time scale. The fast nonspecific formation of this encounter complex may precede a slow (~20 s) specific ligand-binding step associated with folding of the ligand-binding core, which further promotes formation of the loop–loop interaction (~30 s).

To further dissect how preformation and stabilization of tertiary structural elements as well as conformational heterogeneity in the ligand-free form of the riboswitch RNA influences RNA folding trajectories, a G37A/C61U mutant (GSR^{loop}) of the guanine-sensing riboswitch aptamer domain was investigated. In contrast to GSR^{apt} RNA, for which the loop–loop interaction is already present in the ligand-free RNA conformation, the formation of the tertiary loop–loop interaction in GSR^{loop} is absent in the free form, but it can be restored upon addition of Mg^{2+} ions at ratios of $[Mg^{2+}]/[RNA] > 20$. Interestingly, the folding rates exhibited a pronounced dependence on the Mg^{2+} concentration. Apparently, the kinetic barrier for ligand-induced folding of the GSR^{loop} aptamer domain is influenced by Mg^{2+} ions and may arise from both enthalpic and entropic contributions. Electrostatic charge compensation mediated by Mg^{2+} ions appears to be necessary to reduce the enthalpic barrier for native tertiary contacts, especially with respect to the native orientation of the helices P2 and P3, judging by the number of cation binding sites in this region.

Local Base-Pair Dynamics Based on $^1H–^2H$ Exchange Kinetics

Chemical exchange of imino protons in nucleic acids is dependent on the presence of hydrogen bonds to other nucleobases. If imino protons are not protected from chemical exchange by hydrogen bonding, exchange with the solvent is so fast that NMR signals for these imino groups become undetectable. However, under base-pairing conditions,

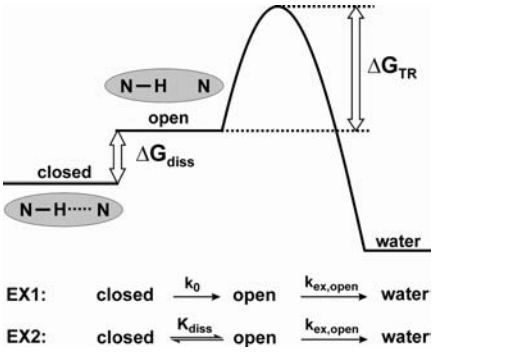

FIGURE 5. Energy diagram describing the imino proton exchange mechanism from the nucleobase in the closed (base-paired) conformation to water. ΔG_{diss}: free energy difference between closed and open conformation of the nucleobase. ΔG_{TR}: free energy barrier for the imino proton transition from the nucleobase in the open state to the water. (Below) Imino proton exchange reaction under EX1 and EX2 conditions. While under EX1 conditions, the exchange process is limited by the base pair opening rate k_0, the exchange process under EX2 conditions is dependent on the equilibrium constant K_{diss} between the closed and the open state of the nucleobase.

exchange is sufficiently slow and imino signals can be observed. Hence, the existence of imino proton signals provides information about the presence of secondary or certain tertiary structural elements in nucleic acids.

Using NMR spectroscopy, the dynamics of uncorrelated base-pair opening events can be characterized by determining imino proton exchange rates with the solvent.[39] Exchange is dependent on temperature, buffer composition, and base-pair stability and is usually within 0.01−1 s. Based on analysis of exchange rates (k_{ex}) under EX2 conditions, changes in the free energy of dissociation (ΔG_{diss}) between the closed and open states of individual nucleobases can be derived (Figure 5). Under EX2 conditions, base pair opening occurs multiple times before imino proton exchange takes place. Therefore, equilibrium between the closed and open state of the nucleobase can be assumed.

Local melting and base pair opening are physiologically important as prerequisites for transcription and replication (dsDNA) and for processes involved in translational regulation (RNA thermometers and riboswitches) and RNA-mediated catalysis.

Chen et al.[40] determined base pair stabilities for the sarcin-ricin domain RNA from the large ribosomal subunit at 10 °C. Thermodynamic stabilities are in the range between 12 and 44 kJ/mol. Interestingly, base pair stabilities were found to be extremely low at the α-sarcin cleavage site so that a base flipping mechanism for α-sarcin cleavage was proposed.

Nonin et al.[41] determined base pair stabilities for an AMP-binding RNA aptamer. Comparison of the free and the AMP-complexed form of the RNA reveals that not only the AMP-binding internal loop but also the adjacent stem residues become stabilized upon AMP binding. Both studies[40,41] show that base pair stabilities are dependent on the nature of the base pairing interaction as well as on the structural context, especially in non-canonical regions of the RNA.

Thermodynamic base pair stabilities have been mapped for a cis-acting, temperature-responsive fourU RNA thermometer from *Salmonella* that regulates gene expression of a small heat shock protein by blocking the SD sequence through base pairing at lower temperatures, thereby hindering translation initiation.[42,43] Thermodynamic stabilities have been analyzed over a broad temperature range, and spatially resolved information on the thermal unfolding process of the RNA helix could be obtained. The wild-type fourU RNA thermometer is stabilized by the extremely stable G14-C25 base pair at low temperatures. At higher temperatures, this base pair becomes significantly destabilized so that global unfolding of the RNA thermometer can occur.

Conclusion

In this Account, we have presented current NMR spectroscopic approaches for characterizing functional dynamics in RNA. Within the present size limit of ~100 nucleotides, NMR yields very detailed structural, kinetic, and thermodynamic data for local as well as global structural transitions in RNA. Through a combination of site-specific mutations, improved isotope-labeling schemes, easy-to-apply segmental labeling strategies, and novel sophisticated NMR parameters, we predict a key role for NMR in understanding the regulatory roles of RNA in prokaryotes and eukaryotes. MD simulations and other kinetic models[44] combined with NMR are powerful tools for mapping the dynamic landscape of RNA.

BIOGRAPHICAL INFORMATION

Harald Schwalbe studied chemistry at Goethe-University of Frankfurt and received his Ph.D. with Prof. Griesinger in 1993. After postdoctoral studies at Oxford with Prof. Dobson, FRS and work on his habilitation, he became an assistant/associate professor at MIT (1999−2001). Since 2002, he has been a Professor of Chemistry at Goethe-University in Frankfurt.

Jörg Rinnenthal received his diploma in biochemistry from the Goethe-University in Frankfurt and completed his Ph.D. in the group of Harald Schwalbe in 2010.

Janina Buck received her diploma in chemistry from the Goethe-University in Frankfurt and completed her Ph.D. in the group of Harald Schwalbe in 2010.

Jan Ferner received his diploma in chemistry from the Goethe-University in Frankfurt and completed his Ph.D. in the group of Harald Schwalbe in 2009. Since 2007, he has been a staff member in this group.

Anna Wacker received her diploma in biochemistry from the Goethe-University in Frankfurt in 2007 and is working on her Ph.D. thesis in the group of Harald Schwalbe.

Boris Fürtig studied biochemistry at the Goethe-University of Frankfurt and received his Ph.D. in the group of Harald Schwalbe in 2007. Afterwards, he carried out postdoctoral studies in the group of Prof. Renée Schroeder at the Max F. Perutz Laboratories in Vienna.

Deutsche Forschungsgemeinschaft (DFG) (Schwerpunktprogramm SPP 1258: Sensory and regulatory RNAs in prokaryotes); Sonderforschungsbereich (SFB) 902. H.S. is member of the Cluster of Excellence: Macromolecular complexes and the Center for Biomolecular Magnetic Resonance (BMRZ).

FOOTNOTES

*To whom correspondence should be addressed. E-mail: schwalbe@nmr.uni-frankfurt.de. Telephone: +49 (0)69/798-29737. Fax: +49 (0)69/798-29515.

REFERENCES

1 Hansel, R.; Foldynova-Trantirkova, S.; Löhr, F.; Buck, J.; Bongartz, E.; Bamberg, E.; Schwalbe, H.; Dötsch, V.; Trantirek, L. Evaluation of Parameters Critical for Observing Nucleic Acids Inside Living Xenopus laevis Oocytes by In-Cell NMR Spectroscopy. *J. Am. Chem. Soc.* **2009**, *131*, 15761–15768.

2 Akke, M.; Fiala, R.; Jiang, F.; Patel, D.; Palmer, A. G., 3rd. Base dynamics in a UUCG tetraloop RNA hairpin characterized by ^{15}N spin relaxation: correlations with structure and stability. *RNA (N.Y.)* **1997**, *3*, 702–709.

3 Shajani, Z.; Varani, G. ^{13}C NMR relaxation studies of RNA base and ribose nuclei reveal a complex pattern of motions in the RNA binding site for human U1A protein. *J. Mol. Biol.* **2005**, *349*, 699–715.

4 Shajani, Z.; Drobny, G.; Varani, G. Binding of U1A protein changes RNA dynamics as observed by C-13 NMR relaxation studies. *Biochemistry* **2007**, *46*, 5875–5883.

5 Al-Hashimi, H. M. Exciting structures. *Science* **2010**, *329*, 1295–1296.

6 Bardaro, M. F.; Shajani, Z.; Patora-Komisarska, K.; Robinson, J. A.; Varani, G. How binding of small molecule and peptide ligands to HIV-1 TAR alters the RNA motional landscape. *Nucleic Acids Res.* **2009**, *37*, 1529–1540.

7 Oberstrass, F. C.; Allain, F. H. T.; Ravindranathan, S. Changes in dynamics of SRE-RNA on binding to the VTS1p-SAM domain studied by C-13 NMR relaxation. *J. Am. Chem. Soc.* **2008**, *130*, 12007–12020.

8 Duchardt, E.; Schwalbe, H. Residue specific ribose and nucleobase dynamics of the cUUCGg RNA tetraloop motif by NMR ^{13}C relaxation. *J. Biomol. NMR* **2005**, *32*, 295–308.

9 Ferner, J.; Villa, A.; Duchardt, E.; Widjajakusuma, E.; Wöhnert, J.; Stock, G.; Schwalbe, H. NMR and MD studies of the temperature-dependent dynamics of RNA YNMG-tetraloops. *Nucleic Acids Res.* **2008**, *36*, 1928–1940.

10 Lipari, G.; Szabo, A. Model-free approach to the interpretation of nuclear magnetic resonance relaxation in macromolecules. 1. Theory and range of validity. *J. Am. Chem. Soc.* **1982**, *104*, 4546–4559.

11 Gherghe, C. M.; Shajani, Z.; Wilkinson, K. A.; Varani, G.; Weeks, K. M. Strong correlation between SHAPE chemistry and the generalized NMR order parameter (S-2) in RNA. *J. Am. Chem. Soc.* **2008**, *130*, 12244–12245.

12 Rinnenthal, J.; Richter, C.; Nozinovic, S.; Fürtig, B.; Lopez, J. J.; Glaubitz, C.; Schwalbe, H. RNA phosphodiester backbone dynamics of a perdeuterated cUUCGg tetraloop RNA from phosphorus-31 NMR relaxation analysis. *J. Biomol. NMR* **2009**, *45*, 143–155.

13 Palmer, A. G., 3rd. NMR characterization of the dynamics of biomacromolecules. *Chem. Rev.* **2004**, *104*, 3623–3640.

14 Tollinger, M.; Skrynnikov, N. R.; Mulder, F. A.; Forman-Kay, J. D.; Kay, L. E. Slow dynamics in folded and unfolded states of an SH3 domain. *J. Am. Chem. Soc.* **2001**, *123*, 11341–11352.

15 Palmer, A. G., 3rd; Kroenke, C. D.; Loria, J. P. Nuclear magnetic resonance methods for quantifying microsecond-to-millisecond motions in biological macromolecules. *Methods Enzymol.* **2001**, *339*, 204–238.

16 Deverell, C.; Morgan, R. E.; Strange, J. H. Studies of chemical exchange by nuclear magnetic relaxation in rotating frame. *Mol. Phys.* **1970**, *18*, 553–559.

17 Johnson, J. E., Jr.; Hoogstraten, C. G. Extensive backbone dynamics in the GCAA RNA tetraloop analyzed using 13C NMR spin relaxation and specific isotope labeling. *J. Am. Chem. Soc.* **2008**, *130*, 16757–69.

18 Kloiber, K.; Spitzer, R.; Tollinger, M.; Konrat, R.; Kreutz, C. Probing RNA dynamics via longitudinal exchange and CPMG relaxation dispersion NMR spectroscopy using a sensitive (13)C-methyl label. *Nucleic Acids Res.* **2011**, *39*, 4340–4351.

19 Zhang, Q.; Sun, X.; Watt, E. D.; Al-Hashimi, H. M. Resolving the motional modes that code for RNA adaptation. *Science (New York, N. Y.)* **2006**, *311*, 653–656.

20 Blackledge, M. Recent progress in the study of biomolecular structure and dynamics in solution from residual dipolar couplings. *Prog. Nucl. Magn. Reson. Spectrosc.* **2005**, *46*, 23–61.

21 Getz, M.; Sun, X.; Casiano-Negroni, A.; Zhang, Q.; Al-Hashimi, H. M. NMR studies of RNA dynamics and structural plasticity using NMR residual dipolar couplings. *Biopolymers* **2007**, *86*, 384–402.

22 Lange, O. F.; Lakomek, N. A.; Fares, C.; Schröder, G. F.; Walter, K. F. A.; Becker, S.; Meiler, J.; Grubmüller, H.; Griesinger, C.; de Groot, B. L. Recognition dynamics up to microseconds revealed from an RDC-derived ubiquitin ensemble in solution. *Science (New York, N.Y.)* **2008**, *320*, 1471–1475.

23 Zhang, Q.; Stelzer, A. C.; Fisher, C. K.; Al-Hashimi, H. M. Visualizing spatially correlated dynamics that directs RNA conformational transitions. *Nature* **2007**, *450*, 1263–1267.

24 Duchardt-Ferner, E.; Weigand, J. E.; Ohlenschläger, O.; Schmidtke, S. R.; Suess, B.; Wöhnert, J. Highly Modular Structure and Ligand Binding by Conformational Capture in a Minimalistic Riboswitch. *Angew. Chem., Int. Ed.* **2010**, *49*, 6216–6219.

25 Mittag, T.; Franzoni, L.; Cavazzini, D.; Schaffhausen, B.; Rossi, G. L.; Günther, U. L. Retinol modulates site-specific mobility of apo-cellular retinol-binding protein to promote ligand binding. *J. Am. Chem. Soc.* **2006**, *128*, 9844–9848.

26 Cavanagh, J.; Fairbrother, W. J.; Palmer, A. G., 3rd; Skelton, N. J. *Protein NMR Spectroscopy. Principles and Practice*; Academic Press: New York, 1996.

27 Jeener, J.; Meier, B. H.; Bachmann, P.; Ernst, R. R. Investigation of exchange processes by two-dimensional NMR spectroscopy. *J. Chem. Phys.* **1979**, *71*, 4546–4553.

28 Schleucher, J.; Wijmenga, S. S. How to detect internal motion by homonuclear NMR. *J. Am. Chem. Soc.* **2002**, *124*, 5881–5889.

29 Latham, M. P.; Zimmermann, G. R.; Pardi, A. NMR Chemical Exchange as a Probe for Ligand-Binding Kinetics in a Theophylline-Binding RNA Aptamer. *J. Am. Chem. Soc.* **2009**, *131*, 5052–5053.

30 Montelione, G. T.; Wagner, G. 2D Chemical-Exchange NMR-Spectroscopy by Proton-Detected Heteronuclear Correlation. *J. Am. Chem. Soc.* **1989**, *111*, 3096–3098.

31 Wenter, P.; Bodenhausen, G.; Dittmer, J.; Pitsch, S. Kinetics of RNA refolding in dynamic equilibrium by ^{1}H-detected ^{15}N exchange NMR spectroscopy. *J. Am. Chem. Soc.* **2006**, *128*, 7579–7587.

32 Sarkar, R.; Vasos, P. R.; Bodenhausen, G. Singlet-state exchange NMR spectroscopy for the study of very slow dynamic processes. *J. Am. Chem. Soc.* **2007**, *129*, 328–334.

33 Fürtig, B.; Richter, C.; Schell, P.; Wenter, P.; Pitsch, S.; Schwalbe, H. NMR-spectroscopic characterization of phosphodiester bond cleavage catalyzed by the minimal hammerhead ribozyme. *RNA Biol.* **2008**, *5*, 41–48.

34 Manoharan, V.; Fürtig, B.; Jäschke, A.; Schwalbe, H. Metal-Induced Folding of Diels-Alderase Ribozymes Studied by Static and Time-Resolved NMR Spectroscopy. *J. Am. Chem. Soc.* **2009**, *131*, 6261–6270.

35 Buck, J.; Li, Y. L.; Richter, C.; Vergne, J.; Maurel, M. C.; Schwalbe, H. NMR Spectroscopic Characterization of the Adenine-Dependent Hairpin Ribozyme. *ChemBioChem* **2009**, *10*, 2100–2110.

36 Fürtig, B.; Buck, J.; Manoharan, V.; Bermel, W.; Jäschke, A.; Wenter, P.; Pitsch, S.; Schwalbe, H. Time-resolved NMR studies of RNA folding. *Biopolymers* **2007**, *86*, 360–383.

37 Buck, J.; Fürtig, B.; Noeske, J.; Wöhnert, J.; Schwalbe, H. Time-resolved NMR methods resolving ligand-induced RNA folding at atomic resolution. *Proc. Natl. Acad. Sci. U.S.A.* **2007**, *104*, 15699–15704.

38 Schlepckow, K.; Wirmer, J.; Bachmann, A.; Kiefhaber, T.; Schwalbe, H. Conserved folding pathways of alpha-lactalbumin and lysozyme revealed by kinetic CD, fluorescence, NMR, and interrupted refolding experiments. *J. Mol. Biol.* **2008**, *378*, 686–698.

39 Gueron, M.; Leroy, J. L. Studies of base pair kinetics by NMR measurement of proton exchange. *Methods Enzymol.* **1995**, *261*, 383–413.

40 Chen, C.; Jiang, L.; Michalczyk, R.; Russu, I. M. Structural energetics and base-pair opening dynamics in sarcin-ricin domain RNA. *Biochemistry* **2006**, *45*, 13606–13613.

41 Nonin, S.; Jiang, F.; Patel, D. J. Imino proton exchange and base-pair kinetics in the AMP-RNA aptamer complex. *J. Mol. Biol.* **1997**, *268*, 359–374.

42 Rinnenthal, J.; Klinkert, B.; Narberhaus, F.; Schwalbe, H. Direct observation of the temperature-induced melting process of the Salmonella fourU RNA thermometer at base-pair resolution. *Nucleic Acids Res.* **2010**, *38*, 3834–3847.

43 Waldminghaus, T.; Heidrich, N.; Brantl, S.; Narberhaus, F. FourU: a novel type of RNA thermometer in Salmonella. *Mol. Microbiol.* **2007**, *65*, 413–424.

44 Cao, S.; Fürtig, B.; Schwalbe, H.; Chen, S. J. Folding Kinetics for the Conformational Switch between Alternative RNA Structures. *J. Phys. Chem. B* **2010**, *114*, 13609–13615.